Research Square

Preprints are preliminary reports that have not undergone peer review.
They should not be considered conclusive, used to inform clinical practice,
or referenced by the media as validated information.

Integrating SSWEI, NpSPI, and NpSPEI to Decode Spatiotemporal Snow Drought Dynamics and Types

Hamidreza Ghasemi
University of Tehran
Javad Bazrafshan
jbazr@ut.ac.ir
University of Tehran
Zahra Aghashariatmadari
University of Tehran

Research Article

Keywords: Snow Drought, SWE, Spatiotemporal Analysis, Climate Warming, Iran

Posted Date: November 12th, 2026

DOI: https://doi.org/10.21203/rs.3.rs-11435077/v1

License: This work is licensed under a Creative Commons Attribution 4.0 International License.
Read Full License

Additional Declarations: No competing interests reported.

Integrating SSWEI, NpSPI, and NpSPEI to Decode Spatiotemporal Snow Drought Dynamics and Types

Hamidreza Ghasemi[1], Javad Bazrafshan[2*], Zahra Aghashariatmadari[2]

[1]MSc Student, Department of Irrigation and Reclamation Engineering, University of Tehran, Karaj, Iran.

[2]Associate Professor, Department of Irrigation and Reclamation Engineering, University of Tehran, Karaj, Iran.

[*] Correspondence to jbazr@ut.ac.ir, Address: College of Agriculture & Natural Resources, University of Tehran, Daneshkadeh Ave., Karaj, Iran; Postal Code: 3158777871. Phone Number: +982632241119)

Abstract

Snow drought, a primary consequence of climate warming, profoundly impacts water resources in mountainous regions. This study monitors, analyzes spatiotemporal trends, and classifies snow droughts (dry, warm, and warm-dry) across Iran. Using daily Snow Water Equivalent (SWE) data and climatic variables from 112 meteorological stations over the 1991–2020 period (during the dominant snow season, November–April), we quantified snow droughts using the non-parametric Standardized SWE Index (SSWEI). To distinguish between drought types, the Non-parametric Standardized Precipitation Index (NpSPI) and the Non-parametric Standardized Precipitation Evapotranspiration Index (NpSPEI) were employed. Stations were categorized into four thermal-elevation climate zones: very cold (>1749 m), cold (1077–1749 m), temperate (596–1077 m), and warm (<596 m). Trend analysis revealed significant declines in SWE across the very cold (-4.93 mm/yr), cold (-1.36 mm/yr), and temperate (-0.57 mm/yr) zones. In the warm zone, the SWE trend was near zero and thus excluded from further analysis. Spatial SSWEI analysis indicated that the most extensive snow droughts occurred in the final years of the study period (2018–2020). Classification analysis demonstrated that compound warm-dry droughts, with a relative frequency of approximately 40%, are the dominant type across all zones, indicating the simultaneous occurrence of precipitation deficits and increased evapotranspiration. In the temperate zone, the frequency of Divergence Type 1 (precipitation surplus but snow drought) increased significantly (about 30%) due to the shift from snow to rainfall. These findings align with global and regional studies highlighting the prevalence of compound droughts and a shift toward a temperature-driven regime under warming scenarios. This study provides a robust methodological framework for monitoring snow droughts in regions with complex topography.

Keywords: Snow Drought; SWE; Spatiotemporal Analysis; Climate Warming; Iran.

1. Introduction

Snowpacks play a vital role as natural water reservoirs in mountainous regions worldwide, including Iran, where approximately half of the territory is mountainous (Sadeqi et al., 2024). Snow drought refers to periods characterized by below-normal snow accumulation, identifiable at monthly, seasonal, and winter scales (Harpold et al., 2017). Unlike conventional droughts, which are primarily defined by precipitation deficits, snow droughts exhibit a dual nature: both precipitation deficits and temperature increases can drive their occurrence (Dierauer et al., 2019). Because snow acts as a natural reservoir that stores winter precipitation and gradually releases it during the warm season, snow deficits can have profound implications for water resources (Huning and AghaKouchak, 2020).

Despite the growing recognition of snow droughts, a universally accepted definition remains elusive, with studies employing various metrics and thresholds, such as April 1 SWE, peak SWE, daily SWE below the climatological median, the Standardized Snow Water Equivalent Index (SSWEI), and percentile thresholds (Li et al., 2026; Harpold et al., 2017). This diversity in definitions leads to discrepancies in the frequency, severity, and timing of identified snow droughts across different analyses. All these studies rely on snowpack SWE to define snow droughts. Unfortunately, snowpack SWE measurement data are unavailable in Iran. Therefore, it is important to note that in this study, the term snow drought specifically refers to snowfall drought, which is quantified based on gauge-measured SWE rather than snowpack SWE.

Snow drought indices are effective tools for evaluating and quantifying the severity of snow drought events in a given region. Several indices have been introduced globally for snow drought monitoring, including the Standardized Snow Melt and Rain Index (SSMRI; Staudinger et al., 2014), the modified Standardized Moisture Anomaly Index incorporating snow dynamics (SZIsnow; Tian et al., 2022; Zhang et al., 2019), the Snow Drought Response Index (SnoDRI; Rasiya Koya et al., 2023), and the Standardized Snow Water Equivalent Index (SSWEI; Colombo et al., 2023; Cowherd et al., 2023; Heldmyer et al., 2023; Huning and AghaKouchak, 2020; Koehler et al., 2022). In this study, the SSWEI was employed to monitor snow droughts.

Studies conducted in Iran indicate a significant decreasing trend in the country's snow cover over recent decades. Ahmadi and Seyedmirzaei (2022), using the MODIS snow cover product from 2003

to 2018, demonstrated that the snow cover area trend was negative across all cold-season months, with the most significant decrease occurring in January at a rate of -0.81% per year. They also identified 2008 as a change point for January snow cover (the coldest month), after which the mean snow cover decreased by approximately 50%. Arkian et al. (2014), analyzing 30 years of data from 28 meteorological stations, reported a declining trend in both the duration and depth of snow cover, particularly at high-elevation and snow-rich stations such as Koohrang and Abali. Montazeri (2018), investigating the frequency of snow codes across 304 synoptic stations in Iran from 1951 to 2010, showed that snow is a low-frequency phenomenon, accounting for less than 2% of 'present weather' observations. Furthermore, Sherafat and Fathnia (2019), analyzing NOAA-AVHRR imagery, documented a decreasing trend in snow cover area in the Zagros region from 1996 to 2015, with the greatest decrease occurring in July and the least in April.

Mountainous and high-elevation regions of Iran, such as the Alborz and Zagros mountain ranges, are highly sensitive to the effects of global warming and climate change due to significant increases in air temperature and altered precipitation patterns. For instance, land surface temperature (LST) has significantly increased in the central Alborz mountainous regions during most months over the past decades (Roshan et al., 2024a; Roshan et al., 2024b). Additionally, shifts in precipitation patterns, including the transition from snow to rain, are highly probable in the Zagros region (Sadrianzadeh et al., 2023). The increasing temperatures and changing precipitation patterns in the Zagros have impacted its agricultural and rangeland areas, necessitating adaptation strategies across various farming and pastoral practices (Tahmasebi et al., 2013). These changes align with global findings on elevation-dependent warming; for example, Pepin et al. (2015) demonstrated that warming rates intensify with altitude in many mountain ranges worldwide, with significant implications for snowmelt and water resources. In Iran, this phenomenon could similarly lead to premature snowmelt and reduced snow storage at high elevations.

The state of snow drought research in Iran reveals a distinct knowledge gap compared to global studies. While internationally, numerous studies have classified snow droughts into dry (simultaneous reduction in SWE, total precipitation, and temperature relative to the mean), warm (reduction in SWE but an increase in total precipitation relative to the mean), and warm-dry (reduction in SWE and total precipitation, coupled with an increase in temperature relative to the mean) (Harpold et al., 2017; Dierauer et al., 2019) and analyzed their long-term trends across various regions globally (Huning and AghaKouchak, 2020; Cowherd et al., 2023; Wang et al., 2025), this topic in Iran was largely neglected

until recently. Despite approximately half of the country's territory being mountainous and a substantial portion of cold-season precipitation being stored as snow in the Alborz and Zagros highlands, a detailed understanding of snow drought behavior was lacking prior to recent studies. Global studies indicate that snow droughts are intensifying in many snow-covered regions worldwide, with their dominant type shifting from dry to warm (Cowherd et al., 2023; Wang et al., 2025). This shift can have profound implications for water resources management, as warm snow droughts are typically accompanied by premature runoff, reduced water storage, and an increased risk of winter flooding (Harpold et al., 2017; Dierauer et al., 2019).

Based on the aforementioned points, the objectives of this study can be summarized as follows:

- Quantifying snow droughts in Iran using the Standardized Snow Water Equivalent Index (SSWEI) and identifying the types of snow droughts (using auxiliary meteorological drought indices).
- Spatiotemporal analysis of snow droughts and investigation of their trend variations in mountainous and snow-covered regions of Iran, particularly the Alborz and Zagros.
- Frequency analysis of the occurrence of snow droughts and their types in Iran.

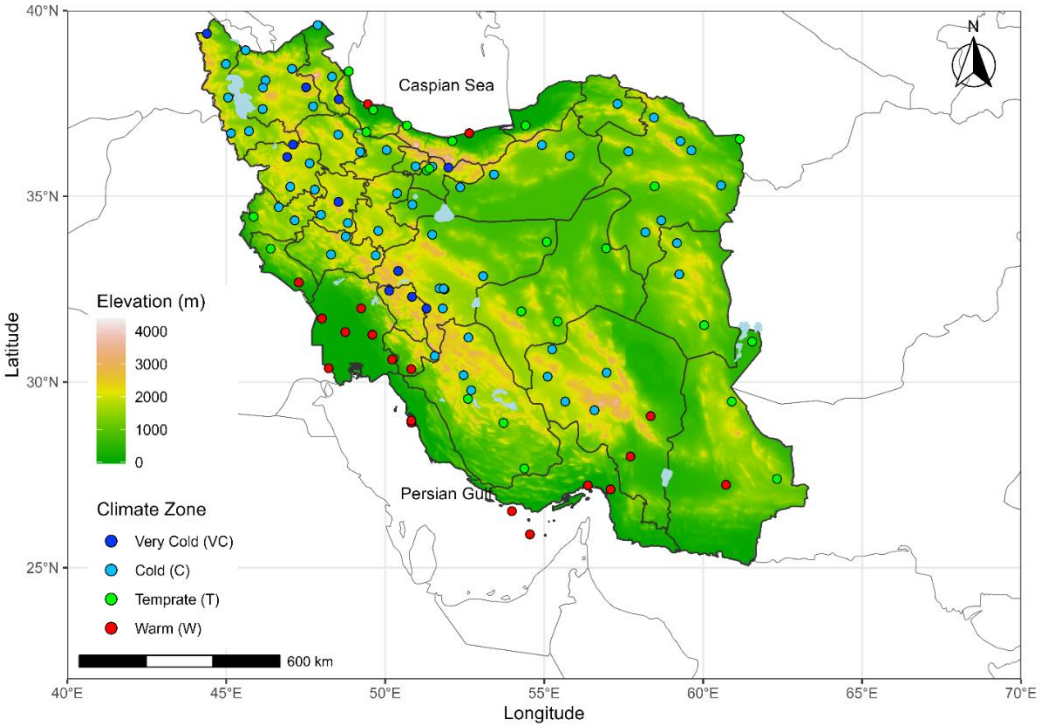
2. Materials and Methods

2.1. Study Area and Data

Iran, covering an area of 1,648,195 km², is situated between 44° and 63.5°E longitude and 25° and 40°N latitude. Located in the arid subtropical belt, it serves as a transitional zone between subtropical and extratropical climates, thereby exhibiting a high degree of climatic diversity. This diversity is driven by the interplay of three factors: geographical location, complex topography, and various synoptic systems (Khalili and Rahimi, 2018). Approximately 83% of the country experiences an arid to semi-arid climate, with a reported mean annual precipitation of about 247 mm (Rahimi et al., 2013). However, a substantial portion of this precipitation is stored as snow at high elevations during the cold season. Roughly half of Iran's landmass is mountainous. The two principal mountain ranges—the Alborz in the north and the Zagros in the west—play a decisive role in shaping precipitation patterns and snow storage. The Alborz range stretches from west to east in northern Iran, is approximately 650 km long, and its northern slopes receive higher precipitation owing to their proximity to the Caspian Sea. The Zagros range, stretching approximately 1,600 km, is located in

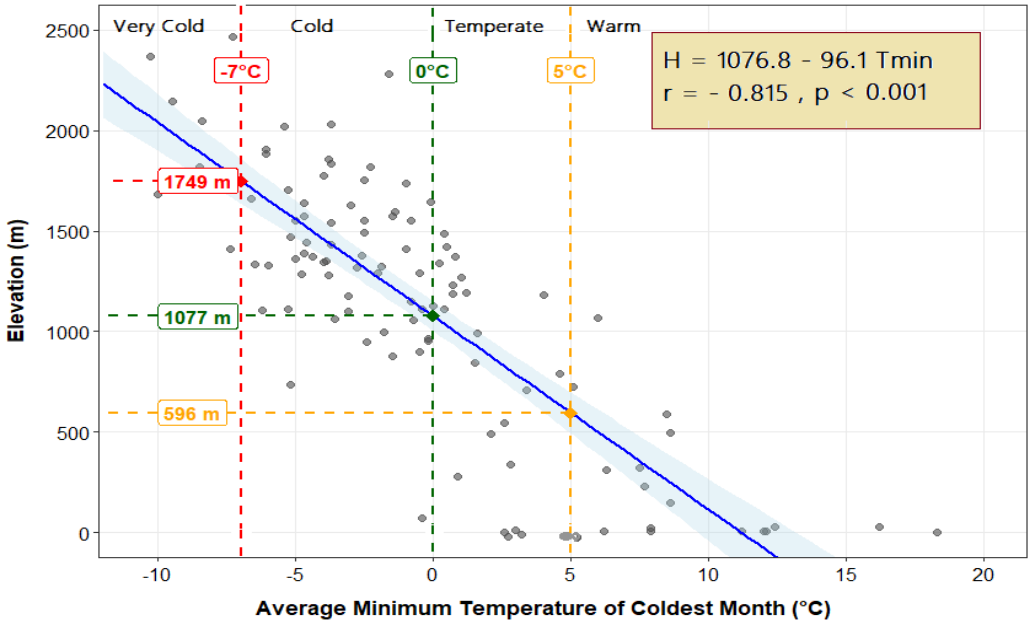
western and southwestern Iran, extending from the northwest to the southeast.

In this study, daily data for five climatic variables—minimum temperature, maximum temperature, mean air temperature, precipitation, and Snow Water Equivalent (SWE)—were obtained from the Iran Meteorological Organization for 142 meteorological stations. The dataset spans the dominant statistical period from 1990 to 2020. Upon data compilation, it was observed that numerous stations contained missing records (data gaps). The temporal distribution and percentage of missing data were assessed for each station. Applying a 10% threshold, stations with less than 10% missing data were selected and subjected to gap-filling procedures. Gap-filling was performed using a nearest-neighbor correlation approach, implemented via the fillgap() function within the hyfo package in the R environment (Xu, 2020). Ultimately, following the gap-filling process, 112 meteorological stations were utilized for this study. Their geographical specifications and thermal climate classifications, based on the Extended De Martonne method (Rahimi et al., 2013), are presented in Table 1, with their spatial distribution illustrated in Figure 1. According to the Extended De Martonne method, the thermal climate classification is based on the mean minimum temperature of the coldest month ($\bar{T}_{min}$): Very Cold climate ($\bar{T}_{min} \leq -7$°C); Cold climate (-7°C $< \bar{T}_{min} \leq 0$°C); Temperate climate (0°C $< \bar{T}_{min} \leq 5$°C); and Warm climate ($\bar{T}_{min} > 5$°C). The distribution of stations across these thermal climates is as follows: 17% (Warm), 20.5% (Temperate), 52.7% (Cold), and 9.8% (Very Cold). In total, 62.5% of the stations are located in Cold and Very Cold climates, where the likelihood of snow is higher compared to other climates. Given the strong relationship between elevation and the minimum temperature of the coldest month, the stations were further categorized by elevation into four corresponding thermal climate zones: Very Cold (elevation > 1,749 m), Cold (elevation between 1,077 and 1,749 m), Temperate (elevation between 596 and 1,077 m), and Warm (elevation < 596 m). These zones represent very high, high, medium, and low elevations, respectively (Figure 2).



144

145 **Figure 1.** Geographical locations and thermal climate zones of the selected stations superimposed on
146 the Digital Elevation Model (DEM) of Iran.



147

148 **Figure 2.** Relationship between elevation and the mean minimum temperature of the coldest month
149 across all selected stations. The shaded band around the regression line represents the 95% confidence
150 interval.

2.2. Determining the Dominant Snow Period

To assess drought conditions at the selected stations in Iran, it is essential to first define the dominant snow period. Figure 3 illustrates the monthly mean number of snow days (with error bars representing ± one standard error) aggregated across all selected stations. As shown in the figure, the mean number of snow days from May through October is nearly zero. The highest frequency of snow days, averaging approximately 3 days per month, occurs in January. Consequently, the results indicate that the dominant snow period in Iran spans six months of the year, from November to April.

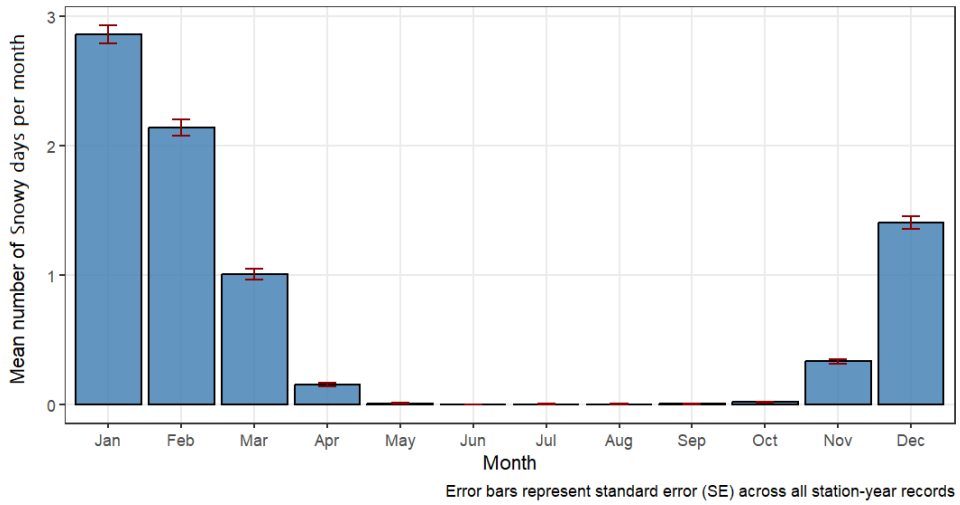


Figure 3. Monthly mean (± standard error) number of snow days aggregated across the selected stations in Iran.

2.3. Drought Indices

In this study, the Standardized Snow Water Equivalent Index (SSWEI) was employed to monitor snow droughts. Classifying snow drought types (i.e., dry, warm, or warm-dry) necessitates additional metrics. These supplementary metrics include total precipitation and mean air temperature. Specifically, the Non-parametric Standardized Precipitation Index (NpSPI) was used as a proxy for total precipitation, and the Non-parametric Standardized Precipitation Evapotranspiration Index (NpSPEI) was used in place of mean air temperature. All three indices were computed using the cumulative values of the respective variables over the dominant snow period (November to April).

2.3.1. Standardized Snow Water Equivalent Index (SSWEI)

In this study, the Standardized Snow Water Equivalent Index (SSWEI) was employed to monitor

snow droughts. This index compares the current Snow Water Equivalent (SWE) at a given location against baseline conditions to identify the presence of a snow drought, though it does not isolate the underlying cause. Snow drought is defined as a deficit in snow, which may stem from either a reduction in total precipitation or a decreased fraction of precipitation occurring as snow (Cowherd et al., 2023).

The calculation of the SSWEI relies on a non-parametric approach, utilizing empirical probabilities rather than fitting a specific theoretical distribution to the SWE data. This method, introduced by Huning and AghaKouchak (2020), has been widely adopted in subsequent studies (Chen et al., 2026). The first step in the Huning and AghaKouchak (2020) framework involves aggregating SWE values over a specified time window (typically 3 months). In this study, rather than a standard 3-month window, the aggregation period was defined as the dominant snow season, spanning from November to April:

$$A_y = \sum_{i=11}^{12} SWE_{i,y-1} + \sum_{i=1}^{4} SWE_{i,y} \quad (1)$$

where SWE_i represents the SWE in month i; A_y is the total aggregated SWE over the dominant snow period; and y denotes the snow season year, covering a 30-year period from 1991 to 2020 in this study. The first term on the right-hand side of Equation (1) accounts for the cumulative SWE in November and December of the preceding year, while the second term represents the cumulative SWE from January to April of the current year. For example, the aggregated SWE for the 1991 snow season (A_{1991}) includes SWE from November and December 1990, as well as January through April 1991.

Subsequently, the empirical probability of each aggregated value is calculated using the Gringorten plotting position formula (Gringorten, 1963):

$$P(A_y) = \frac{y - 0.44}{n + 0.12} \quad (2)$$

where i is the rank of the aggregated value among all sorted values, and n is the sample size (total number of study years). This formula was selected for its suitability in handling Gumbel distributions and hydrological datasets that contain zero values (Gringorten, 1963).

Finally, the SSWEI is derived by transforming the empirical probability into a standard normal distribution, as follows (Huning and AghaKouchak, 2020; Chen et al., 2026):

$$SSWEI(A_y) = \phi^{-1}[P(A_y)] \quad (3)$$

where $\phi^{-1}$is the inverse standard normal distribution function. The SSWEI value can be interpreted as the standardized deviation from the long-term mean snow (Huning and AghaKouchak, 2020). Table 2 provides the classification thresholds for snow drought severity based on SSWEI values (Shrestha et al., 2021). SSWEI values below -1 indicate drought conditions, values between -1 and 1 denote normal conditions, and values greater than 1 indicate wet conditions.

Table 2. Thresholds and descriptions of standard drought index categories (McKee et al., 1993)

Category	Wet spell	Normal	Drought
Moderate	+1.0 to +1.5 (W1)	-1.0 to +1.0 (N)	-1.0 to -1.5 (D1)
Severe	+1.5 to +2.0 (W2)		-1.5 to -2.0 (D2)
Extreme	≥+2.0 (W3)		≤-2.0 (D3)

2.3.2. Non-parametric Standardized Precipitation Index (NpSPI)

The Standardized Precipitation Index (SPI) is one of the most widely applied and validated drought monitoring indices globally, originally introduced by McKee et al. (1993) to monitor drought conditions in Colorado. The sole required input for calculating the SPI is monthly precipitation data. A key characteristic of the SPI is its flexibility to be computed across multiple time scales. While vegetation dynamics are primarily influenced by shorter time scales (e.g., 3 months), surface and groundwater resources respond to longer accumulation periods.

In this study, a methodology analogous to that of the SSWEI was adopted to compute the SPI. Rather than employing varying moving time windows, a fixed six-month window spanning November to April (the dominant snow period) was utilized. The cumulative precipitation for this period was calculated, and the non-parametric Gringorten plotting position formula (Equation 2) was applied to determine the empirical probabilities of the seasonal precipitation totals. Finally, following Equation 3, the empirical probabilities were transformed into a standard normal distribution, yielding the Non-parametric Standardized Precipitation Index (NpSPI). The classification thresholds provided in Table 2 were used to categorize the NpSPI values.

2.3.3. Non-parametric Standardized Precipitation Evapotranspiration Index (NpSPEI)

The Standardized Precipitation Evapotranspiration Index (SPEI), introduced by Vicente-Serrano et al. (2010), is established as a climatic water balance index. This index relies on quantifying the climatic water balance and requires monthly precipitation and potential evapotranspiration (PET) data for its computation. The climatic water balance equation is defined as:

$$D_i = P_i - PET_i \quad (4)$$

where P_i and PET_i denote precipitation and potential evapotranspiration, respectively; D_i is their difference; and i represents the month index.

Various empirical and physical equations are available for estimating PET, and the calculation of the SPEI is not restricted to a specific method. When only air temperature data are available, the Thornthwaite (1948) method is typically employed. Conversely, when a broader range of climatic variables is accessible, more physically robust and accurate approaches, such as the Hargreaves-Samani or Penman-Monteith methods, are preferred. In this study, due to the unavailability of solar radiation data, the Hargreaves-Samani method (Hargreaves and Samani, 1985) was adopted to estimate monthly PET.

Traditionally, the SPEI is computed by calculating D for each month, applying a moving sum over different accumulation periods, and fitting a parametric probability distribution. In this study, rather than employing moving time windows of varying lengths, a fixed six-month window spanning November to April (the dominant snow season in Iran) was applied. The cumulative water balance for this period was calculated, and the non-parametric Gringorten plotting position formula (Equation 2) was utilized to determine the empirical probabilities. Subsequently, according to Equation 3, the empirical probabilities of the cumulative water balance were transformed into standard normal variables, yielding the Non-parametric Standardized Precipitation Evapotranspiration Index (NpSPEI). The thresholds outlined in Table 2 were used to classify the NpSPEI values.

2.4. Spatiotemporal Analysis of Drought Indices

A comprehensive spatiotemporal analysis of drought necessitates integrating statistical methods to quantify snow drought severity (as detailed in Section 2.3.1), trend tests to evaluate temporal dynamics, and geostatistical techniques for spatial interpolation. The methodological framework for this analysis

is outlined in the following subsections.

2.4.1. Trend Analysis

The Mann-Kendall (MK) test and the Sen's slope estimator are among the most widely applied non-parametric methods for trend analysis in hydroclimatic time series (Mann, 1945; Kendall, 1975; Sen, 1968). These techniques are extensively utilized in climatological and hydrological studies because they do not require the data to follow a normal distribution and are highly robust against outliers.

2.4.1.1. Mann-Kendall Test

The Mann-Kendall (MK) test is a non-parametric method used to detect monotonic increasing or decreasing trends in time series. The null hypothesis of this test assumes that the data are randomly ordered and independent. The MK test S statistic is defined as follows:

$$S = \sum_{k=1}^{n-1} \sum_{j=k+1}^{n} \mathrm{sgn}(X_j - X_k) \tag{5}$$

where sgn()is the sign function, defined as:

$$\mathrm{sgn(x)} = \begin{cases} 1 & \text{if x} > 0 \\ 0 & \text{if x} = 0 \\ -1 & \text{if x} < 0 \end{cases} \tag{6}$$

The expected value of S is zero ($E[S] = 0$), and its variance is given by:

$$\sigma^2 = \frac{n(n-1)(2n+5) - \sum_{j=1}^{p} t_j \left(t_j - 1\right)\left(2t_j + 5\right)}{18} \tag{7}$$

where p is the number of tied groups and t_j is the number of data points in the j-th tied group. The standardized Z statistic is computed as:

$$Z = \begin{cases} \dfrac{S-1}{\sigma} & \text{if } S > 0 \\ 0 & \text{if } S = 0 \\ \dfrac{S+1}{\sigma} & \text{if } S < 0 \end{cases} \tag{8}$$

A positive value of Z indicates an increasing trend, while a negative value indicates a decreasing trend. It is important to note that the presence of autocorrelation in hydroclimatic data can overestimate the variance of the S statistic, thereby increasing the probability of detecting a false trend. To address this issue, Hamed and Rao (1998) proposed a variance correction approach based on the effective sample

size. In this method, the variance of the S statistic is adjusted using a correction factor that accounts for the serial correlation of ranks. To correct the variance in the MK formula, the effective sample size is calculated using the following equation:

$$n_{HR}^{*} = \frac{n}{1 + \frac{2}{n(n-1)(n-2)} \sum_{i=1}^{n-1} (n-i)(n-i-1)(n-i-2)\, \rho_s(i)} \quad (9)$$

where $\rho_s(i)$ is the autocorrelation function of the ranks of the observations. Subsequently, the corrected variance is obtained from $V^{*}(S) = V(S) \cdot \frac{n}{n_{HR}^{*}}$, and the Z statistic is recalculated using this updated variance. This method is implemented in the modifiedmk package in R via the mmkh() function (Patakamuri and O'Brien, 2021).

2.4.1.2. Sen's Slope Estimator

The Sen's slope estimator (Sen, 1968) is a non-parametric method used to determine the magnitude of a trend. This technique utilizes the median of all possible slopes between data pairs and is highly robust against outliers (Sen, 1968; Theil, 1950). To calculate Sen's slope, the slope for each data pair (X_j, X_k), where $j > k$, is first determined as follows:

$$Q_i = \frac{X_j - X_k}{j - k} \quad , \text{ for } i = 1,2, \dots, N \quad (10)$$

Subsequently, the median of the Q_i values (Sen's slope) is obtained according to the following equation:

$$Q_{med} = \begin{cases} Q_{(N+1)/2} & \text{if } N \text{ is odd} \\ \frac{1}{2}(Q_{N/2} + Q_{(N+2)/2}) & \text{if } N \text{ is even} \end{cases} \quad (11)$$

The sign of Q_{med} indicates the direction of the trend, and its value represents the slope of the trend line (change per unit time).

2.4.2. Spatial Analysis and Interpolation

To generate continuous drought maps from discrete station data, statistical and geostatistical interpolation methods are applied within a GIS environment (Hosseini et al., 2021). Selecting an appropriate interpolation method is a strategic decision in spatial drought analysis and depends on the specific conditions of each region. Hybrid approaches combining statistical and geostatistical methods have been widely recommended in numerous studies. Notable examples include the regression-kriging

method (Nadi et al., 2012) and the regression-inverse distance weighting method (Tanır Kayıkçı and Zengin Kazancı, 2016; Chen et al., 2014). Among various geostatistical techniques, kriging (particularly ordinary and simple kriging) is generally regarded as a precise and standard method, provided that the data allow for reliable variogram modeling. Another widely used alternative is the Inverse Distance Weighting (IDW) method. IDW is a powerful, simple, and computationally efficient option that performs exceptionally well, especially in regions with sparse station networks or complex topography where variogram modeling is challenging (Mohammadi Ghaleni et al., 2024).

In this study, a hybrid gradient method based on multivariate linear regression and IDW was employed to generate drought zoning maps. The independent variables in the regression model include elevation (H), longitude (X), and latitude (Y). First, a multivariate linear regression model is established between the climatic variable (Z) and the geographical attributes as follows:

$$\hat{Z} = a + bX + cY + dH \tag{12}$$

where a is the regression constant, and b, c, and d are the regression coefficients. Subsequently, the residuals ($\varepsilon = Z - \hat{Z}$) are calculated at the station locations, and these residuals are interpolated using the IDW method to produce a residual map. The mathematical formulation of the IDW method is as follows:

$$\hat{\varepsilon}_i = \sum_{i=1}^{n} \frac{\varepsilon_i}{d_i^p} \Big/ \sum_{i=1}^{n} \frac{1}{d_i^p} \tag{13}$$

where d_i is the distance between the unknown point and the i-th station, and p is the power parameter (typically set to 2). A key characteristic of the IDW method is that it precisely reproduces the residual values at the exact station locations. Finally, the interpolated residual map is added back to the regression trend surface (Equation 12) to correct the spatial distribution of drought severity. This hybrid approach has been extensively utilized by Khalili (1997) for mapping climatic variables across Iran.

2.5. Frequency Analysis of SSWEI Classes vs. NpSPI and NpSPEI

By comparing the Standardized Snow Water Equivalent Index (SSWEI, representing snow drought) with either the Non-parametric Standardized Precipitation Index (NpSPI, representing meteorological precipitation drought) or the Non-parametric Standardized Precipitation Evapotranspiration Index (NpSPEI, representing climatic water balance drought), four distinct scenarios emerge (Figure 4):

- Positive Alignment (PA) (Wet precipitation/water balance and wet snow): Both the NpSPI/NpSPEI and SSWEI indices exhibit positive values (a surplus in both). This indicates that both seasonal precipitation/water balance and snow are above normal. This scenario is considered ideal for water resources.
- Negative Alignment (NA) (Dry precipitation/water balance and dry snow): Both indices are negative (a deficit in both). This signifies that both seasonal precipitation/water balance and snow are below normal. This represents the worst-case scenario for water resource deficits.
- Divergence Type 1 (DT.1) (Wet precipitation/water balance, but dry snow): The NpSPI/NpSPEI is positive (above-normal precipitation/water balance), while the SSWEI is negative (snow deficit). This pattern typically reflects warm winters where a portion of the precipitation falls as rain rather than snow, or where snowmelt occurs prematurely.
- Divergence Type 2 (DT.2) (Dry precipitation/water balance, but wet snow): The NpSPI/NpSPEI is negative (below-normal precipitation/water balance), whereas the SSWEI is positive (snow surplus). This rare scenario typically occurs during exceptionally cold winters, where limited precipitation is fully preserved as snow due to negligible evaporation and minimal melt losses.

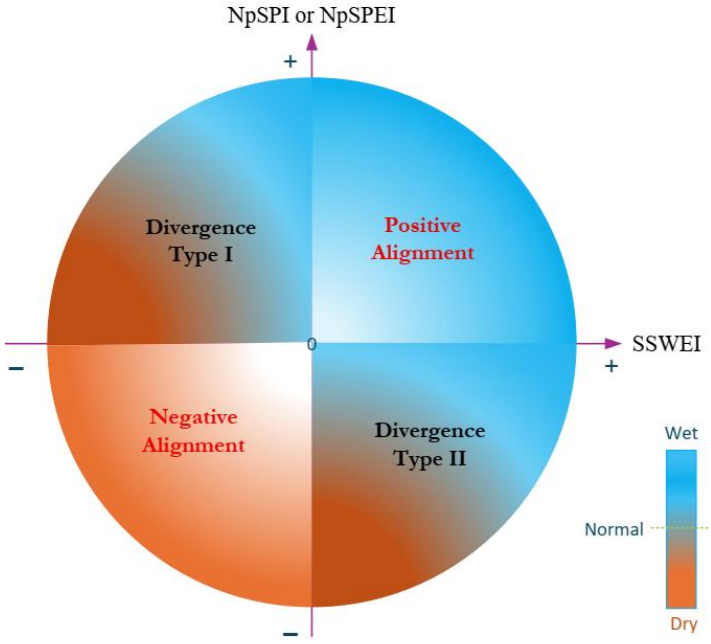


Figure 4. The four possible alignment and divergence states between SSWEI and NpSPI/NpSPEI.

Based on these four states, it is evident that snow droughts can only occur under one of two conditions: Negative Alignment (NA) or Divergence Type 1 (DT.1). Figure 5 illustrates the classification framework for the three specific types of snow drought (Dry, Warm, and Warm-Dry). According to this flowchart, the drought classification follows a step-by-step evaluation of the indices:

Step 1: The SSWEI is evaluated first. If the condition SSWEI < 0 is not met, it indicates that no snow drought has occurred.

Step 2: If SSWEI < 0 is satisfied, the NpSPI is then evaluated.

- If NpSPI ≥ 0, the NpSPEI is examined. In this case, if NpSPEI < 0, a Warm snow drought is identified; otherwise, no drought is recorded.
- If NpSPI < 0, the values of NpSPEI and NpSPI are compared. If NpSPEI <NpSPI, the event is classified as a Warm-Dry snow drought. Otherwise, it is classified as a dry snow drought.

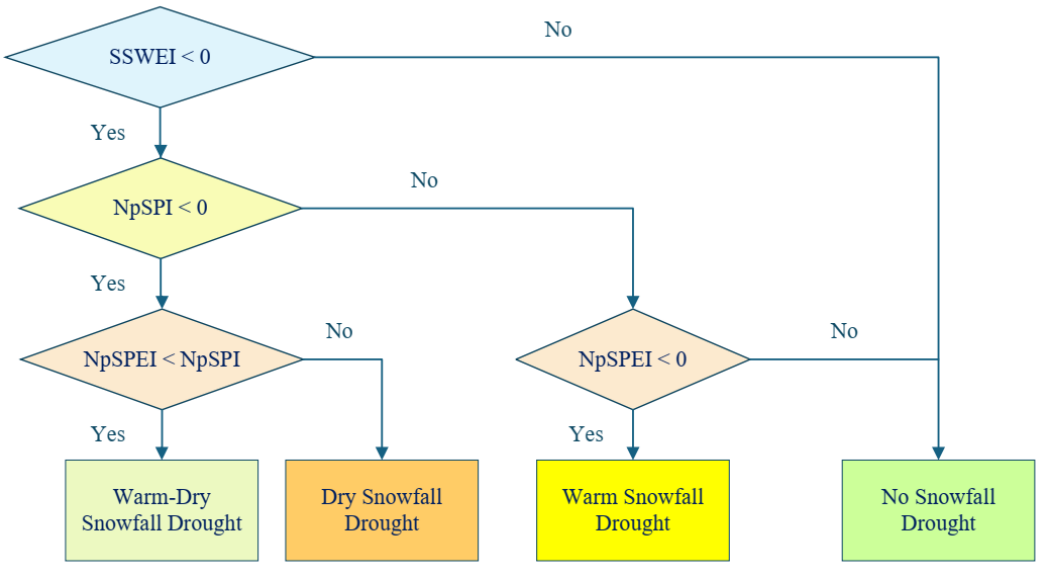


Figure 5. Flowchart for determining snow drought types using the SSWEI, NpSPI, and NpSPEI indices.

3. Results

3.1. Spatial Distribution of Snow Duration, Precipitation, and SWE

Figure 6 illustrates the spatial distribution of four climatic variables across Iran: the long-term mean annual number of snow months, Snow Water Equivalent (SWE), total precipitation, and the ratio of

SWE to total precipitation. As shown in Figure 6, the long-term mean number of snow months in Iran ranges from zero in the central desert and along the southern and southwestern coasts to approximately 8 months in the high elevations of the Alborz and Zagros ranges and the northwestern mountains. The mean SWE varies from zero to approximately 900 mm in the central Zagros highlands, although in most snow-covered regions of the country, the annual SWE is less than 200 mm. Annual precipitation is below 250 mm over a large portion of the country; however, it reaches 1,000 to 1,200 mm in the Alborz and Zagros highlands, and up to 2,000 mm along the Caspian coastal strip. The SWE-to-total precipitation ratio reaches up to approximately 0.8 across the country, though it remains below 0.2 over vast areas. This ratio reaches 0.4 in the relatively high mountains of the Alborz and Zagros, the northeastern mountains, and the Kerman region, and approaches 0.8 in the central Alborz, central Zagros, and northwestern highlands. Based on the data from the 112 selected stations, the highest values of this ratio were recorded at Koohrang (0.67) and Abali (0.57).

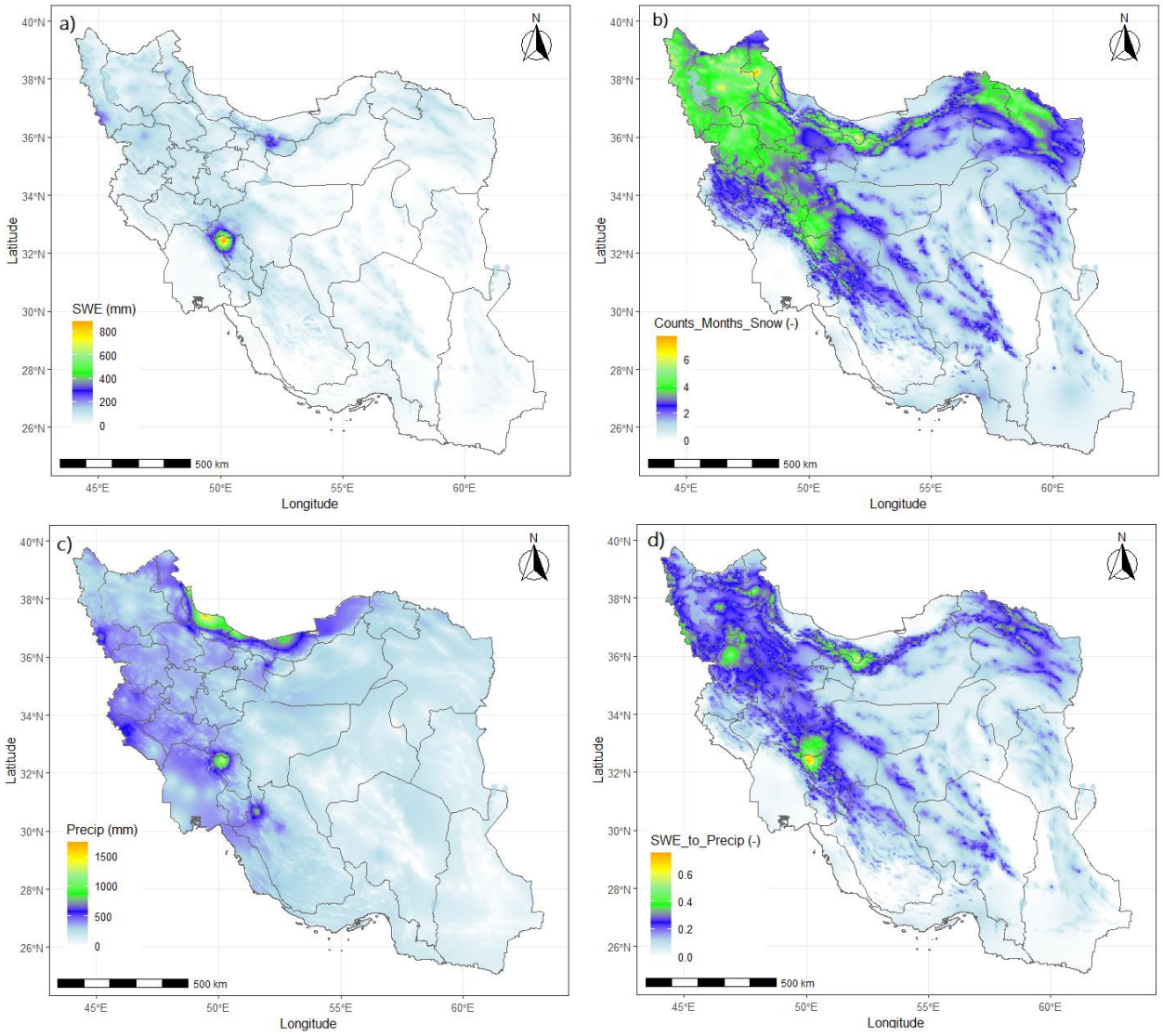


Figure 6. Spatial distribution of the mean annual number of snow months (a), Snow Water Equivalent (SWE) (b), total precipitation (c), and the ratio of SWE to total precipitation (d) across Iran.

3.2. Trend Analysis of SWE in Thermal Climates

The time series of mean Snow Water Equivalent (SWE) from 1991 to 2020 across the four thermal climates (Figure 7) exhibit a significant decreasing trend in the Very Cold, Cold, and Temperate zones. Specifically, the Very Cold climate, characterized by the highest mean SWE (~300 mm), experienced the most pronounced absolute decline (-4.93 mm/yr, $R^2 = 0.379$). This was followed by the Cold (-1.36 mm/yr, $R^2 = 0.405$) and Temperate (-0.57 mm/yr, $R^2 = 0.216$) zones. In contrast, the Warm zone not only exhibits the lowest SWE values (near zero) but also demonstrates a statistically

insignificant and nearly flat trend. Furthermore, the wide shaded bands (representing ± 1 standard deviation) across all climates, particularly in the Very Cold and Cold zones, indicate high interannual snow variability. Even in the Warm and Temperate zones, isolated extreme spikes are observed (e.g., the 2008 anomaly in the Warm zone).

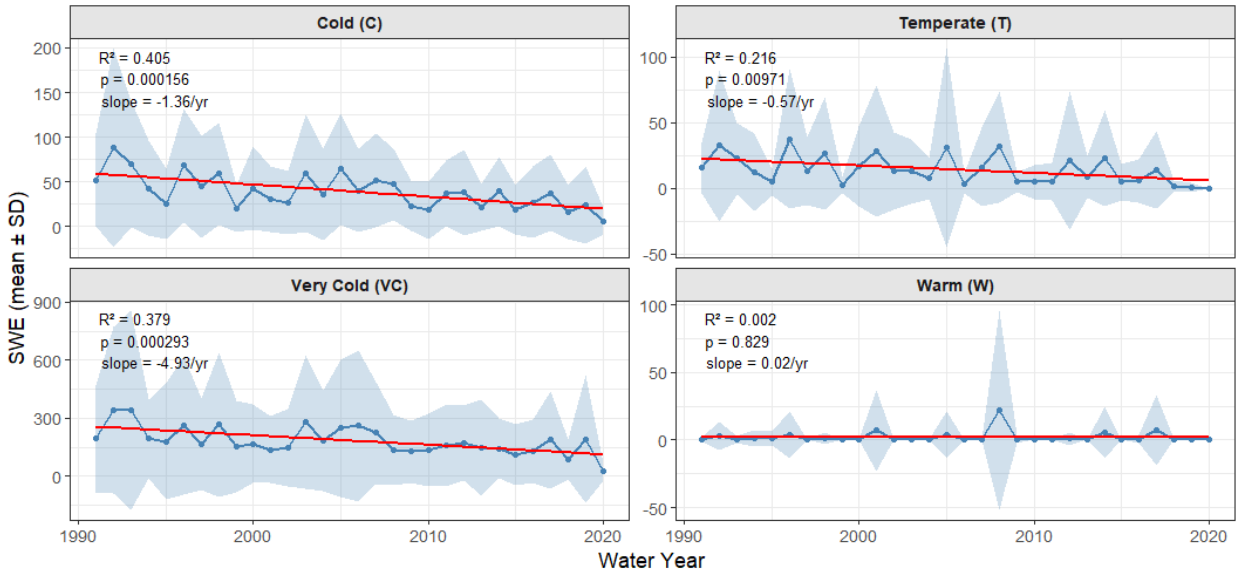


Figure 7. Temporal variations and trends in mean Snow Water Equivalent (SWE) across the four thermal climate zones. The shaded areas around the mean represent the standard deviation of SWE for stations located within each respective climate zone.

Beyond linear trend analysis, the monotonic (linear/non-linear) trends of the SWE time series were evaluated. As detailed in Table 1, the mean SWE trends in the Very Cold, Cold, and Temperate zones are statistically significant and negative, whereas no significant trend is detected in the Warm zone. The Mann-Kendall (MK) S-statistic is negative across all climate zones; however, the trends are statistically significant at the 95% confidence level only for the Very Cold ($Z = -3.50, p < 0.001$), Cold ($Z = -3.53, p < 0.001$), and Temperate ($Z = -2.53, p = 0.01$) zones. In the Warm zone ($Z = -1.03, p = 0.30$), the trend is not statistically significant. Based on Sen's slope estimator, the magnitude of the decline is greatest in the Very Cold zone (-4.41 mm/yr), followed by the Cold (-1.38 mm/yr) and Temperate (-0.55 mm/yr) zones; Sen's slope is approximately zero in the Warm zone. Therefore, we conclude that: (1) the decline in SWE is more severe and definitive in colder climates, diminishing in magnitude towards warmer zones; and (2) the downward trends in the Very Cold, Cold, and Temperate zones are significant at the 5% level. These findings are consistent with the linear trend

slopes presented in Figure 7.

Table 1. Trend analysis of mean Snow Water Equivalent (SWE) time series (1991–2020) across different thermal climate zones of Iran.

Climate Zone	Mann-Kendall Test			Sen's Slope Test			
	S Statistic	Z Statistic	p-value	Sen's Slope (mm/yr)	Lower 95% CI	Upper 95% CI	p-value
Very Cold	-197	-3.50	0.00	-4.41	-7.06	-2.10	0.00
Cold	-199	-3.53	0.00	-1.38	-2.13	-0.64	0.00
Temperate	-143	-2.53	0.01	-0.55	-1.01	-0.16	0.01
Warm	-55	-1.03	0.30	0.00	-0.04	0.00	0.30

3.3. Snow Drought Monitoring

In this study, snow droughts were evaluated using the Standardized Snow Water Equivalent Index (SSWEI) over the dominant snow period in Iran (November to April) across 112 selected stations spanning four thermal climate zones. According to the SSWEI heatmap (Figure 8), the Very Cold climate zone (e.g., Abali and Koohrang) exhibits the highest interannual variability. The 1990s were characterized by moderate to extreme wet conditions (e.g., 1993 and 1997), the 2000s shifted toward normal and mildly dry conditions, and the 2010s—particularly the period from 2014 to 2020—were dominated by severe and extreme droughts, marking a structural break in the snow regime of the country's highest-elevation regions. The Cold climate zone (containing the highest station density, e.g., Tabriz and Zanjan) experienced a similar yet less intense pattern. Scattered wet periods during the 1990s gave way to normal to moderate drought conditions in the 2000s. From the mid-2010s onward, severe and exceptional droughts expanded across all stations, with 2018 and 2020 recording as dry snow years at many locations. The Temperate climate zone (e.g., Gorgan and Shiraz) displays a more muted heatmap, as snow has become a low-frequency phenomenon. While the 1990s featured a few distinct snow years, normal conditions dominated the 2000s and 2010s, with only scattered wet events observed (e.g., 2008 in Gorgan and Rasht). Stations such as Lar and Saravan recorded no snow days, rendering snow drought monitoring inapplicable at those locations. The Warm climate zone (e.g., Ahvaz, Abadan, Bandar Abbas, Bushehr, Bam, and Kish) is almost entirely devoid of data, as significant snow does not occur. The notable exception is Bandar Anzali, which maintains a relatively consistent snow regime due to marine humidity and its mid-latitude positioning.

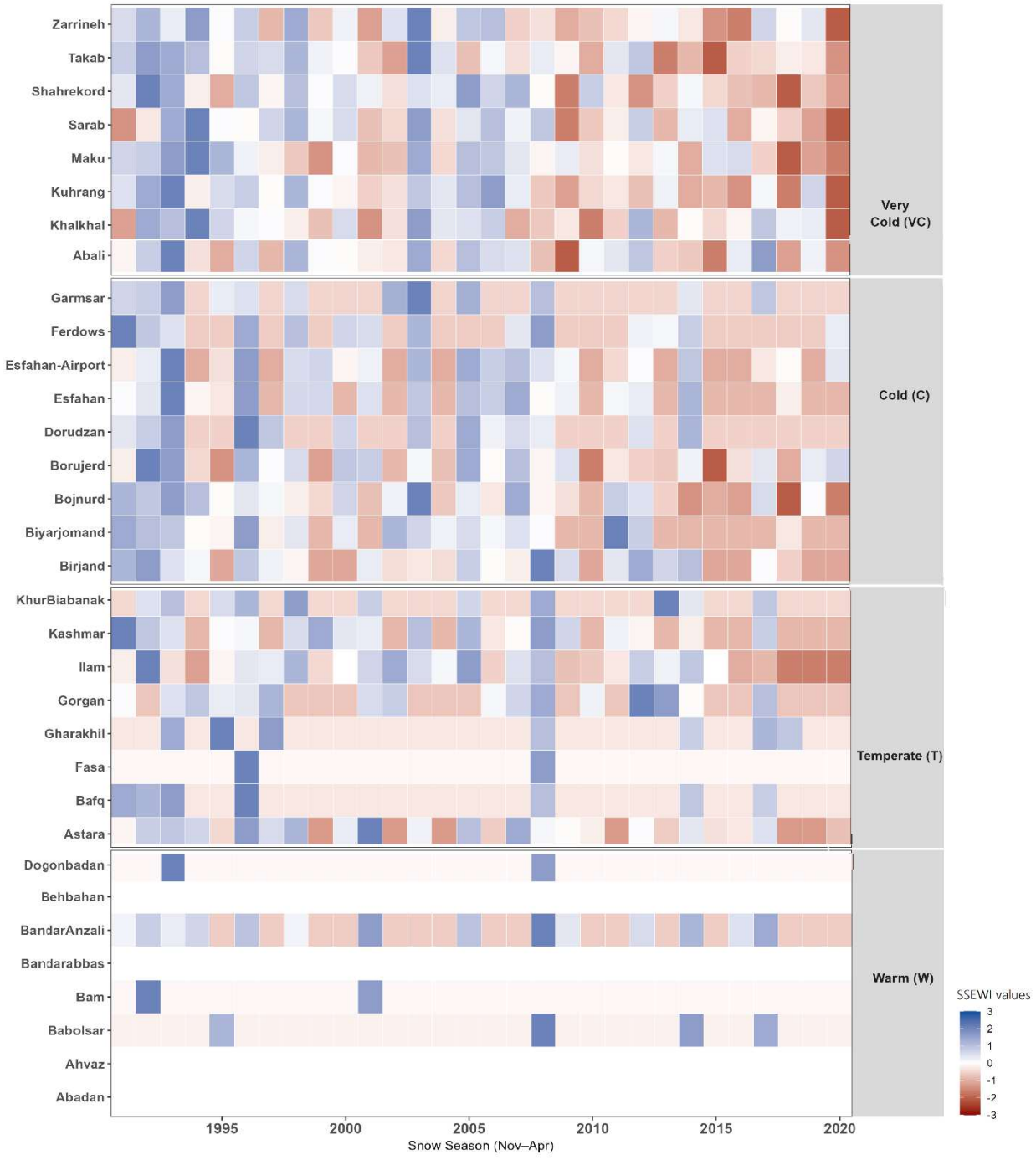


Figure 8. Heatmap of the Standardized Snow Water Equivalent Index (SSWEI) for the selected meteorological stations across the four thermal climate zones during the 1991–2020 period (each year denotes a snow season, encompassing the six-month period from November to April).



Figure 9. Median (± standard deviation) of the Standardized Snow Water Equivalent Index (SSWEI) aggregated across all stations within each of the four thermal climate zones.

To compare the Standardized Snow Water Equivalent Index (SSWEI) across all stations within each of the four thermal climate zones, the median (± standard deviation) SSWEI was computed and is presented in Figure 9. The analysis reveals highly heterogeneous patterns for SSWEI across the four thermal climate zones from 1991 to 2020. Colder zones (particularly the Very Cold zone) experienced the highest annual fluctuations and spatial dispersion (indicated by long error bars). Following a wet period during the 1990s and early 2000s, these regions shifted sharply toward drought in the latter years of the study period (particularly 2015–2020), with 2020 recording the most severe drought in the Very Cold zone (median ≈ -2). Conversely, the Temperate and, notably, Warm zones exhibited much greater stability, remaining largely within the normal range throughout the study period. These findings suggest an overarching drying trend over the last decade, the severity of which is far more critical and perilous in cold climates where water resources are heavily reliant on snowmelt.

3.4. Spatial Analysis of Snow Droughts

Figure 10 illustrates the spatial distribution of the SSWEI over the 1991–2020 period. The SSWEI

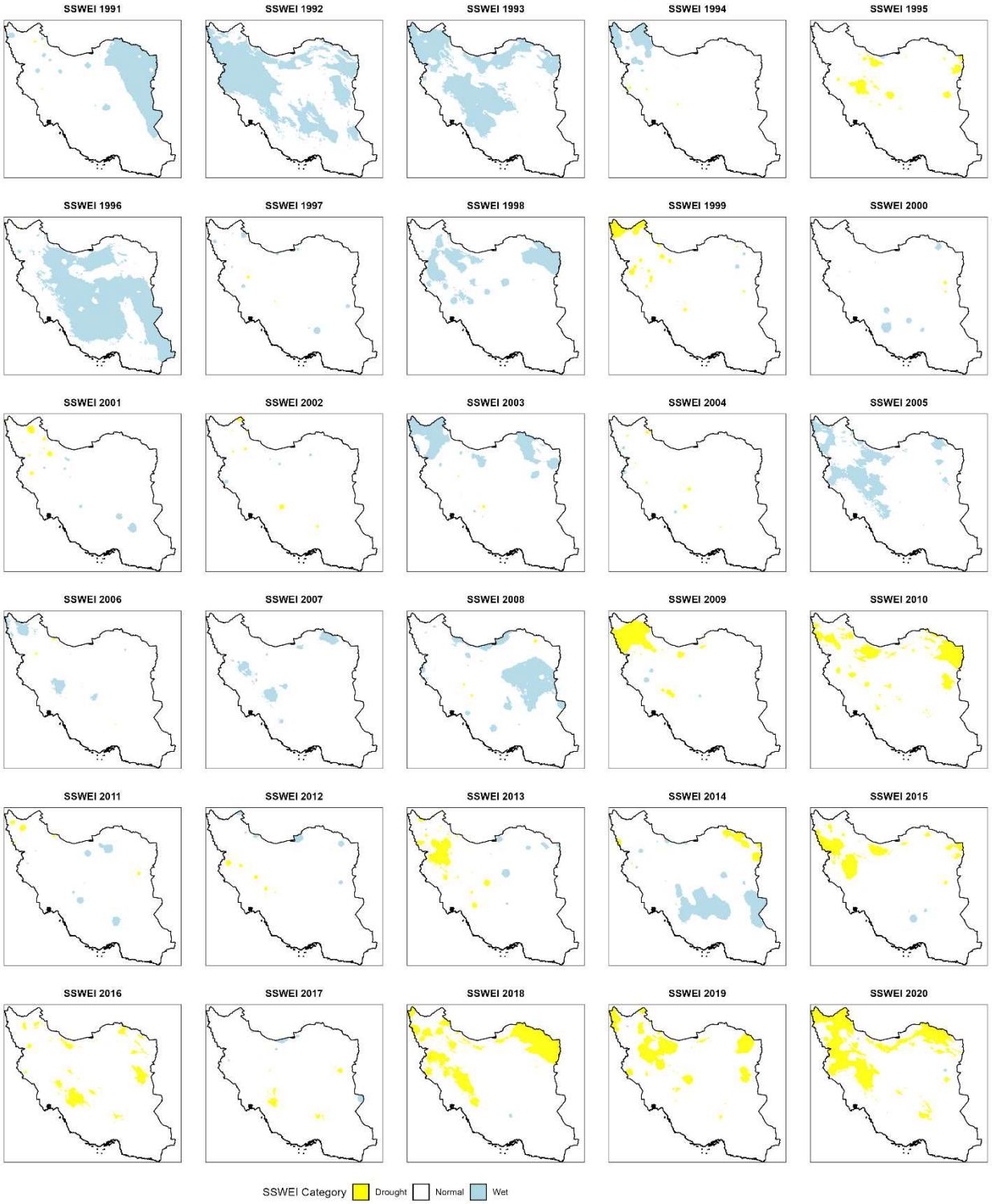


Figure 10. Spatial distribution of the Standardized Snow Water Equivalent Index (SSWEI) (drought: < -1; normal: between -1 and 1; wet: > 1) during the snow season (November to April) across Iran over the 1991–2020 period.

distribution pattern across the three consecutive decades indicates a gradual transition from widespread wet conditions to pervasive droughts. During the 1990s, the years 1992, 1993, and particularly 1996 exhibited the most extensive spatial coverage of wet conditions throughout the entire study period. In 1996, large portions of the central and western regions experienced highly favorable snow reserves, whereas droughts during this decade appeared primarily as small, scattered patches in 1995 and 1999. During the 2000s, normal conditions prevailed. Scattered droughts were observed mostly in the western and central regions in 2001, 2004, and 2008. Conversely, wet conditions occurred as small, isolated, and scattered patches in the central and northern regions during 2005 and 2008. From the 2010s onward, the spatial pattern of drought underwent a noticeable shift. In 2010, 2013, and 2015, drought patches expanded across the north and east, with this transition peaking in the final years of the decade. Specifically, in 2018, 2019, and 2020, snow droughts became extensive and continuous, covering vast areas across the northern, northeastern, eastern, and central regions. By 2020, nearly the entire eastern and northern half of the region was confronted with severe snow drought.

Figure 11 illustrates the percentage of the total study area occupied by each SSWEI category (drought, normal, and wet) for each snow year. Based on the stacked bar chart, it is evident that the normal category (white bars) consistently accounts for the largest proportion throughout the entire 30-year period (typically exceeding 70–80% of the area). This indicates that intermediate (normal) conditions have been the dominant state across the region. Notably, 1996 stands out as the wettest year of the period, with nearly 47% of the study area classified as wet (blue bars), followed by 1992 (~38%) and 1993 (~30%).

A key finding from this figure is the gradual yet continuous increase in the proportion of drought conditions (yellow bars) from the 2010s onward. While the drought extent rarely exceeded 5% during the 1990s and 2000s, it reached approximately 10–15% in 2009 and 2010. This trend culminated in 2018 (~15%), 2019 (~11%), and 2020 (~18%). Ultimately, the year 2020 recorded the highest percentage of area affected by snow drought over the entire study period.

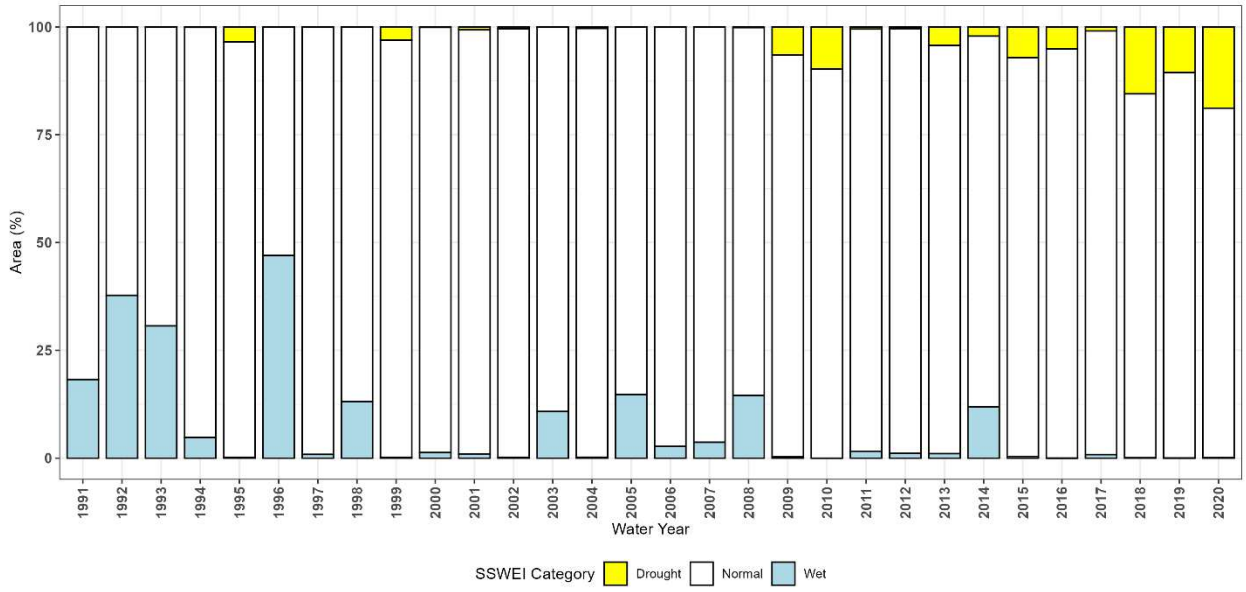


Figure 11. Stacked bar chart (percentage area) of the SSWEI drought, normal, and wet categories during the 1991–2020 period in Iran.

3.5. Frequency Analysis of SSWEI Classes vs. Other Drought Indices

The concurrent analysis of the Standardized Snow Water Equivalent Index (SSWEI) alongside the Non-parametric Standardized Precipitation Index (NpSPI) and the Non-parametric Standardized Precipitation Evapotranspiration Index (NpSPEI) provides valuable insight into the role of temperature in climate change, as it distinguishes whether snow deficits stem from reduced precipitation or from warming-induced precipitation phase shifts (i.e., snow converting to rain). This comparative analysis was conducted on the drought index time series across the Very Cold, Cold, and Temperate climate zones. In the Warm climate zone, such an analysis was not feasible due to the absence or rarity of snow events.

Overall, as illustrated in Figure 12, the frequency distribution pattern of the SSWEI relative to both the NpSPI and NpSPEI is remarkably similar and consistent. In colder climates (Very Cold and Cold), Positive Alignment (PA) and Negative Alignment (NA) states exhibit the highest frequencies (approximately 30–35%), indicating a strong synchronicity and correlation between snow droughts and meteorological precipitation/climatic water balance droughts in these regions. Conversely, transitioning toward the Temperate climate, the frequency of the PA state decreases sharply (to approximately 18%), while the frequency of Divergence Type 1 (DT.1) increases significantly (to

approximately 30%). Consequently, in the Temperate climate zone, DT.1 becomes the most prevalent state, likely attributable to the more prominent role of evapotranspiration in these regions. Furthermore, Divergence Type 2 (DT.2) exhibits the lowest frequency across all climate zones (approximately 15–18%). Moreover, the relatively large standard deviations (particularly within the Temperate climate for the PA and DT.1 states) highlight the high spatial variability and heterogeneity of these states among the stations within each climate zone.

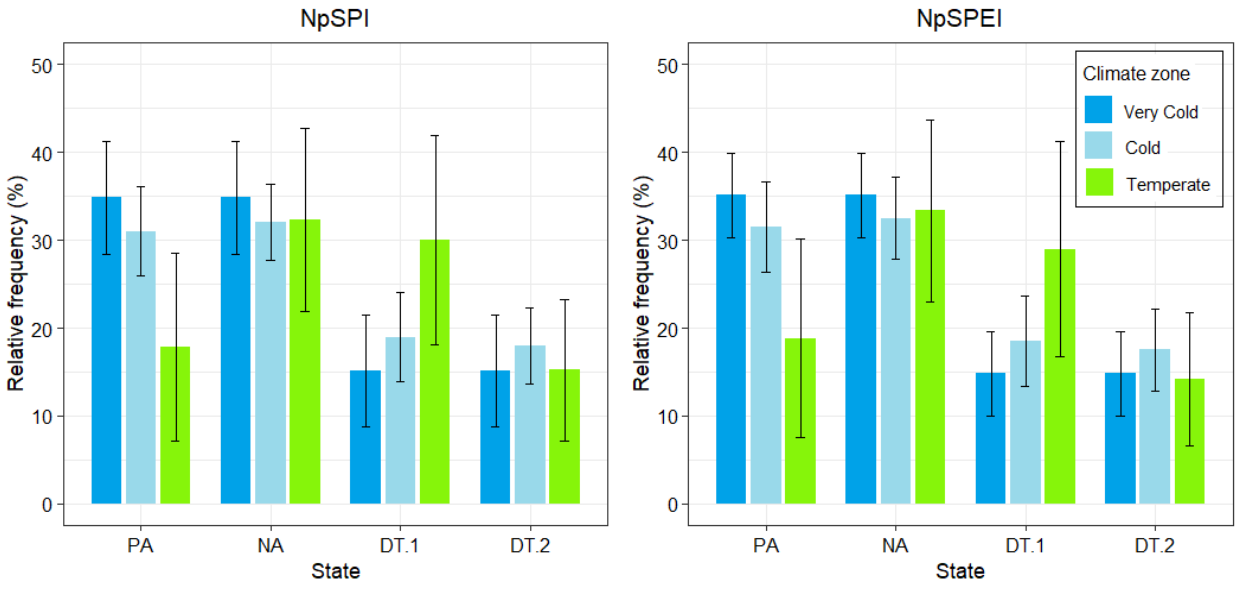


Figure 12. Mean (± standard deviation) relative frequency (%) of Positive Alignment (PA), Negative Alignment (NA), Divergence Type 1 (DT.1), and Divergence Type 2 (DT.2) between the SSWEI and NpSPEI, and the SSWEI and NpSPI, across the thermal climate zones of Iran.

3.6. Frequency Analysis of Snow Drought Types

Figure 13 presents the mean (± standard deviation) relative frequency of the three snow drought types (Dry, Warm, and Warm-Dry) across the Very Cold, Cold, and Temperate climate zones. The most prominent finding of this figure is the overwhelming and absolute dominance of Warm-Dry droughts across all climate zones. Specifically, the relative frequency of this drought type is approximately 40%, whereas the frequency of purely Dry or purely Warm droughts remains notably low across all three climates, at approximately 10% to 11%. Another notable observation is the high uniformity and convergence of the pattern among the different climate zones, implying that there is no significant difference in the distribution of these three drought types across the Very Cold, Cold, and Temperate climates. This finding indicates that, irrespective of the baseline thermal conditions of each climate

zone, whenever a snow drought occurs in Iran, it predominantly manifests as the simultaneous occurrence of precipitation deficits (dryness) and temperature increases (warming). Overall, this figure emphasizes that snow drought in Iran is a compound phenomenon in which increased evapotranspiration (driven by warming) and decreased precipitation act concurrently, thereby exacerbating each other's effects.

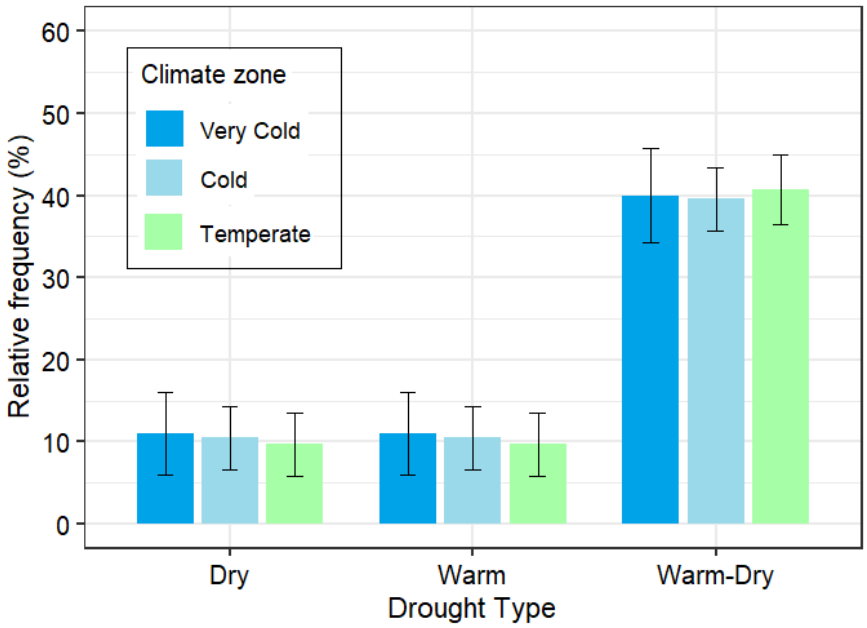


Figure 13. Mean (± standard deviation) relative frequency (%) of snow droughts across the thermal climate zones of Iran.

4. Discussion

The findings of this study—demonstrating a significant decline in Snow Water Equivalent (SWE) across all climate zones, most notably the steepest decline in the Very Cold climate (−4.93 mm/yr)—align closely with a recent study based on ERA5-Land reanalysis data in Iran (Hajivand Paydari et al., 2026). That study indicates that the temperature during the dominant snow season (November–April) in Iran has increased at a rate of approximately 0.67°C per decade, and peak SWE has decreased at a rate of 10.3 mm per decade, while precipitation has exhibited no significant trend. This indicates a structural shift in the mechanism of snow drought in Iran: a transition from a precipitation-deficit regime to a temperature-driven regime. This diagnosis is fully consistent with our results, as across all four climates, the share of compound warm-dry droughts is far greater than that of purely dry droughts, implying that temperature (rather than precipitation deficit alone) has become the primary

limiting factor for snow reserves. MODIS-based assessments (snow cover persistence) further confirm that temperature accounts for approximately 58% of the reduction in Iran's snow cover, whereas precipitation accounts for roughly 42% (Karimi and Sarbazvatan, 2025).

The absolute dominance of compound warm-dry droughts (~40%) across all zones is physically consistent with the three-tier snow drought classification framework (dry, warm, and warm-dry) proposed by Dierauer et al. (2019). In fact, warm-dry droughts result from the simultaneous occurrence of precipitation deficits and abnormally high temperatures. Dierauer et al. (2019) note that compound warm and dry conditions typically generate the most severe snow droughts, as the effects of reduced precipitation and accelerated melt processes exacerbate each other. The high proportion of this drought type in the present study indicates that snow drought in Iran is not a single-factor product but rather the result of the synergistic interaction between moisture stress and thermal stress. This finding is consistent with the global-scale results of Huning and AghaKouchak (2020), who demonstrated that in climate transition zones and lower elevations, the effect of increasing temperature on reducing snow reserves can surpass the influence of precipitation variability. From a physical mechanism perspective, increasing temperatures exacerbate snow drought through two pathways: first, the phase shift of precipitation from solid to liquid (rain), which directly reduces snow accumulation; and second, the acceleration of existing snowmelt, which shortens the lifespan of the snow reserve. The continuation of the warming trend during Iran's cold season has activated both pathways simultaneously, consequently raising the frequency of warm-dry droughts to abnormally high levels.

The rapid rate of SWE decline in the Very Cold climate (−4.93 mm/yr), which appears counterintuitive at first glance (the coldest region experiences the greatest decline), can be explained by the Elevation-Dependent Warming (EDW) phenomenon (Pepin et al., 2015). EDW refers to the increase in warming rates with increasing elevation, driven by factors such as snow-albedo feedback and water vapor feedback. MODIS observations in Iran show that the mean elevation of snow cover has shifted to higher altitudes at a rate of approximately 29 m per year (a total of about 638 m), which is equivalent to a warming rate of about 0.07 to 0.09°C per year (Karimi and Sarbazvatan, 2025). At high elevations in the Very Cold climate, positive snow-albedo feedback is highly decisive: a reduction in snow cover decreases the surface albedo, causing the land to absorb more solar energy, which raises local temperatures and accelerates the melt of remaining snow (Liu et al., 2026). Because these regions initially hold the largest snow volumes, the potential for this positive feedback is maximized there.

Therefore, although the Very Cold climate has the highest baseline SWE, it exhibits the most sensitive response to warming due to these mechanisms. Furthermore, studies have shown that the deposition of light-absorbing particles such as black carbon in the Alborz highlands reduces snow albedo and, combined with rising temperatures, intensifies snowmelt and exacerbates the vulnerability of these regions (Norooz-Valashedi and Noroozian-Rostami, 2026).

In the Temperate climate, the share of Divergence Type 1 (DT.1)—where precipitation is normal or above normal but a snow drought occurs—reaches approximately 30%. This pattern exactly matches the classic definition of a warm snow drought provided by Harpold et al. (2017) and Dierauer et al. (2019): total precipitation is near or above average, but due to higher temperatures, the fraction of precipitation falling as snow is reduced, or snow melts prematurely, resulting in an SWE deficit. In the Temperate climate, winter temperatures often hover near the 0°C threshold (the rain-snow transition boundary); therefore, even slight warming can cause non-linear and dramatic shifts in the solid-to-liquid precipitation ratio. This explains why warm snow droughts are far more common in the Temperate climate than in colder climates. Recent observations in Iran also confirm this; at snow-dominated stations, wet periods have been accompanied by significant temperature increases, such that a larger proportion of precipitation during the warm season has fallen as rain rather than recharging snow reserves (Motamedi et al., 2023). Thus, the high frequency of DT.1 in the Temperate climate is not statistical noise but a clear signal of a change in the hydrological response of these regions to global warming.

The methodological framework employed in this study (integrating SSWEI, NpSPI, and NpSPEI) offers significant advantages. First, the SSWEI and its non-parametric version (based on the Gringorten empirical probability) are the most suitable options for regions like Iran that face sparse ground station networks and complex topography. The standardized SWE deficit assessment framework developed by Huning and AghaKouchak (2020) enables the comparison of snow droughts across different climates. Second, using NpSPEI (instead of raw temperature) as a thermal stress proxy provides a more precise physical meaning for separating warm-dry droughts from dry ones. When NpSPEI is more negative than NpSPI, it signifies that the increase in atmospheric water demand (potential evapotranspiration) exceeds what can be explained by precipitation deficits alone; this discrepancy is a clear indicator of the involvement of thermal stress.

5. Conclusion

This study investigated and classified snow droughts in Iran using data from 112 meteorological stations over the 1991–2020 period. The results revealed a significant decreasing trend in Snow Water Equivalent (SWE) across the Very Cold, Cold, and Temperate climate zones, with the decline being most pronounced in colder climates. The analysis of snow drought types using the index alignment matrix demonstrated that Warm-Dry droughts (a combination of precipitation deficits and thermal stress) are the most prevalent drought type across all snow-covered climate zones in Iran. Furthermore, in the Temperate climate, the divergence state (wet precipitation conditions but snow drought) accounts for a substantial proportion, primarily due to increasing temperatures and the shift from snow to rainfall. These findings are consistent with recent studies in Iran indicating a regime shift in snow droughts from precipitation-driven to temperature-driven. Overall, it can be concluded that snow droughts in Iran are strongly influenced by global warming, and the methodological framework presented in this study provides a precise approach for identifying compound droughts. This framework can be effectively utilized in water resource management and climate change adaptation planning in the mountainous and snow-covered regions of the country.

Acknowledgments

All meteorological data used in this study were obtained from the Iran Meteorological Organization, for which we are grateful.

Contributions

Hamidreza Ghasemi: Conceptualization, Methodology, Investigation, Formal analysis, Resources, Software, Writing - Review & Editing. **Javad Bazrafshan and Zahra Aghashariatmadari**: Conceptualization, Investigation, Supervision, Writing - Review & Editing.

Ethics declarations

Conflict of interest

The authors declare no competing interests.

Funding Declaration

The authors declare no funding.

References

Ahmadi, M., and Seyedmirzaei, Z. (2022). Snow Cover Variability in the Cold Period of the Year in Iran Based on MODIS Measurements. Iranian Journal of Remote Sensing and GIS 14, 59-72.

Arkian, F., Karimkhani, M., and Taheri, H. (2014). Variability and trends in the duration and depth of snow cover in Iran in thirty years. Journal of Earth Science & Climatic Change, 5, 1.

Chen, C., Zhao, N., Yue, T., & Guo, J. (2014). A generalization of inverse distance weighting method via kernel regression and its application to surface modeling. *Arabian Journal of Geosciences*, 7(9), 6623–6633. https://doi.org/10.1007/s12517-013-1084-7

Chen, H., Wang, S., Zhu, P. and AghaKouchak, A. (2026). Winter wheat yield sensitivity to snow drought is increasing across the Northern Hemisphere. Nat Food 7, 174–184.

Colombo, N., Guyennon, N., Valt, M., Salerno, F., Godone, D., Cianfarra, P., et al. (2023). Unprecedented snow-drought conditions in the Italian Alps during the early 2020s. Environmental Research Letters, 18, 074014.

Cowherd, M., Ruby Leung, L., and Girotto, M. (2023). Evolution of global snow drought characteristics from 1850 to 2100. Environmental Research Letters, 18, 064043.

Dierauer, J. R., Allen, D. M., and Whitfield, P. H. (2019). Snow drought risk and susceptibility in the western United States and southwestern Canada. Water Resources Research, 55, 3076-3091.

Gringorten, I.I., 1963. A plotting rule for extreme probability paper. Journal of Geophysical Research 68, 813-814.

Hajivand Paydari, S., Saligheh, M., Alijani, B., and Karbalaei, A. (2026). Assessing the Sensitivity of Iran's Snow Water Equivalent to Temperature and Precipitation and Its Implications for Snow Drought Types (Dry, Warm, and Warm-Dry). *Applied Research in Geographical Sciences* (In Press).

Hamed, K. H., & Rao, A. R. (1998). A modified Mann-Kendall trend test for autocorrelated data. Journal of Hydrology, 204(1–4), 182–196.

Hargreaves, G. H., & Samani, Z. A. (1985). Reference crop evapotranspiration from temperature. Applied Engineering in Agriculture, 1(2), 96–99. **https://doi.org/10.13031/2013.26773**

Harpold, A. A., Dettinger, M., and Rajagopal, S. (2017). Defining snow drought and why it matters. Eos, 98, 15-17.

Heldmyer, A. J., Bjarke, N. R., and Livneh, B. (2023). A 21st-century perspective on snow drought in the Upper Colorado River Basin. Journal of the American Water Resources Association, 59, 396-415.

Hosseini, A., Ghavidel, Y., Mohammad Khorshiddoust, A., & Farajzadeh, M. (2021). Spatio-temporal analysis of dry and wet periods in Iran by using Global Precipitation Climatology Center-Drought Index (GPCC-DI). Theoretical and Applied Climatology, 143(3), 1035–1045.

Huning, L. S., and AghaKouchak, A. (2020). Global snow drought hot spots and characteristics. Proceedings of the National Academy of Sciences, 117, 19753-19759.

Karimi, N., and Sarbazvatan, A. (2025). Robust assessment of snow persistence dynamics in Iran (2002–2024) using MODIS satellite imagery and multi-source evaluation. *Remote Sensing Applications: Society and Environment* **40**, 101806.

Kendall, M. G. (1975). Rank Correlation Methods (4th ed.). Charles Griffin, London.

Khalili, A. (1997). Synthesis proceeding of integrated water plan of Iran. Jamab Consulting Engineering Co., Climate Section, The Ministry of Energy, Tehran, Iran.

Khalili, A., and Rahimi, J. (2018). Climate. In "The Soils of Iran" (M. H. Roozitalab, H. Siadat and A. Farshad, eds.), pp. 19-33. Springer International Publishing, Cham.

Koehler, J., Dietz, A.J., Zellner, P., Baumhoer, C.A., Dirscherl, M., Cattani, L., Vlahović, Ž., Alasawedah, M.H., Mayer, K., Haslinger, K., Bertoldi, G., Jacob, A., and Kuenzer, C., (2022). Drought in Northern Italy: Long Earth Observation Time Series Reveal Snow Line Elevation to Be Several Hundred Meters Above Long-Term Average in 2022. Remote Sensing 14.

Liu, X., Huang, R., Zhang, W., Wu, S., Pang, H., & Hou, S. (2026). Elevation-dependent warming at high altitudes in the westerlies-dominated Tibetan Plateau. *Communications Earth & Environment*.

Mann, H. B. (1945). Nonparametric tests against trend. Econometrica, 13(3), 245–259.

McKee, T. B., Doeskin, N. J., and Kleist, J. (1993). The relationship of drought frequency and duration to time scales. In "Proceedings of the eighth conference on applied climatology", pp. 179–184. American Meteorological Society, Anaheim, CA.

Mohammadi Ghaleni, M., Sharafi, S., & Sadat-Noori, M. (2024). Propagation pathways from meteorological to agricultural drought in different climatic basins in Iran. Environmental Science and Pollution Research, 31(49), 59625–59641

Montazeri, M. (2018). Frequency analysis of snowfall in Iran over the past decades. *Iran-Water Resources Research* **14**, 279-283.

Motamedi, A., Gohari, A., and Haghighi, A. T. (2023). Three-decade assessment of dry and wet spells change across Iran, a fingerprint of climate change. *Scientific Reports* **13**, 2888.

Nadi, m., Jamei, M., Bazrafshan, J., and Janatrostami, S. (2012). Evaluation of Different Methods for Interpolation of Mean Monthly and Annual Precipitation Data (Case Study: Khuzestan Province). *Physical Geography Research* **44**, 117-130.

Norooz-Valashedi, R., and Noroozian-Rostami, M. (2025). Ecohydrological analysis of black carbon effects on accelerated snowmelt in the Alborz highlands using remote sensing and statistical modeling. *Journal of Natural Environment* **78**, 253-266.

Patakamuri, S. K., & O'Brien, N. (2021). modifiedmk: Modified Versions of Mann Kendall and Spearman's Rho Trend Tests (Version 1.6) [R package]. CRAN

Pepin, N., Bradley, R.S., Diaz, H.F., Baraer, M., Caceres, E.B., Forsythe, N., Fowler, H., Greenwood, G., Hashmi, M.Z., Liu, X.D., Miller, J.R., Ning, L., Ohmura, A., Palazzi, E., Rangwala, I., Schöner, W., Severskiy, I., Shahgedanova, M., Wang, M.B., Williamson, S.N., Yang, D.Q., 2015. Elevation-dependent warming in mountain regions of the world. Nature Climate Change 5, 424.

Rahimi, J., Ebrahimpour, M., and Khalili, A. (2013). Spatial changes of Extended De Martonne climatic zones affected by climate change in Iran. Theoretical and Applied Climatology 112, 409-418.

Rasiya Koya, S., Kar, K. K., Srivastava, S., Tadesse, T., Svoboda, M., and Roy, T. (2023). An autoencoder-based snow drought index. Scientific Reports, 13, 20664.

Roshan, G., Sarli, R., Ghanghermeh, A., Taherizadeh, M., and Niknam, A. (2024a). Using satellite-derived land surface temperatures to clarify the spatiotemporal warming trends of the Alborz Mountains in northern Iran. Journal of Mountain Science 21, 449-469.

Roshan, G., Sarli, R., Grab, S. W., Nasiri, V., and Socha, J. (2024b). Elevational trends of land surface temperature in the Alborz Mountains within the context of global warming. Stochastic Environmental Research and Risk Assessment 38, 1721-1739.

Sadeqi, A., Irannezhad, M., Bahmani, S., Jelodarlu, K.A., Varandili, S.A., Pham, Q.B., (2024). Long-Term Variability and Trends in Snow Depth and Cover Days Throughout Iranian Mountain Ranges. Water Resources Research 60, e2023WR035411.

Sadrianzadeh, M., Kharazi, H. G., Eslami, H., Fathian, H., and Telvari, A. (2023). Impact of Climate Change on the Precipitation Trend and Phase in Snow-Dominated Mountain Basins (Central Zagros Mountains, Iran). Water Resources 50, 48-57.

Sen, P. K. (1968). Estimates of the regression coefficient based on Kendall's tau. Journal of the American Statistical Association, 63(324), 1379–1389.

Sherafat, M., and Fathnia, A. (2019). Monitoring the Spatial-Temporal Changes of Snow Surfaces in Zagross Mountains using NOAA-AVHRR Images. The Journal of Spatial Planning and Geomatics 23, 173-194.

Shrestha, R. R., Bonsal, B. R., Bonnyman, J. M., Cannon, A. J., and Najafi, M. R. (2021). Heterogeneous snowpack response and snow drought occurrence across river basins of northwestern North America under 1.0°C to 4.0°C global warming. Climatic Change 164.

Staudinger, M., Stahl, K., and Seibert, J. (2014). A drought index accounting for snow. Water Resources Research, 50, 7861-7872.

Tahmasebi, A., Ehlers, E., and Schetter, C. (2013). CLIMATE CHANGE AND MOUNTAIN PASTORALISM — THE SHAHSEVAN OF NORTHWEST IRAN. Erdkunde 67, 309-323.

Tanır Kayıkçı, E., & Zengin Kazancı, S. (2016). Comparison of regression-based and combined versions of Inverse Distance Weighted methods for spatial interpolation of daily mean temperature data. Arabian Journal of Geosciences, 9(17). https://doi.org/10.1007/s12517-016-2723-0

Theil, H. (1950). A rank-invariant method of linear and polynomial regression analysis. Proceedings of the Koninklijke Nederlandse Akademie van Wetenschappen, 53, 386–392, 521–525, 1397–1412.

Thornthwaite, C. W. (1948). An Approach toward a Rational Classification of Climate. Geographical Review 38, 55-94.

Tian, L., Zhang, B., and Wu, P. (2022). A global drought dataset of standardized moisture anomaly index incorporating snow dynamics (SZIsnow) and its application in identifying large-scale drought events. Earth System Science Data, 14, 2259-2278.

Vicente-Serrano, S. M., Beguería, S., and López-Moreno, J. I. (2010). A multiscalar drought index sensitive to global warming: The standardized precipitation evapotranspiration index. Journal of Climate 23, 1696-1718.

Wang, C., Li, Z., Guyennon, N., Chen, Y., Li, Y., Liang, Q., and Di, Y. (2025). Patterns of snow drought under climate change: From dry to warm dominance. Geophysical Research Letters, 52, e2025GL114641.

Xu, Y. (2020). hyfo: Hydrology and Climate Forecasting R Package for Data Analysis and Visualization. http://yuanchao-xu.github.io/hyfo/.

Zhang, B., Xia, Y., Huning, L. S., Wei, J., Wang, G., and AghaKouchak, A. (2019). A framework for global multicategory and multiscalar drought characterization accounting for snow processes. Water Resources Research, 55, 9258-9278.